CrossMark

# Application of a linked stress release model in Corinth Gulf and Central Ionian Islands (Greece)

Ourania Mangira[1] · Georgios Vasiliadis[2] · Eleftheria Papadimitriou[1]

**Abstract** Spatio-temporal stress changes and interactions between adjacent fault segments consist of the most important component in seismic hazard assessment, as they can alter the occurrence probability of strong earthquake onto these segments. The investigation of the interactions between adjacent areas by means of the linked stress release model is attempted for moderate earthquakes ($M \geq 5.2$) in the Corinth Gulf and the Central Ionian Islands (Greece). The study areas were divided in two subareas, based on seismotectonic criteria. The seismicity of each subarea is investigated by means of a stochastic point process and its behavior is determined by the conditional intensity function, which usually gets an exponential form. A conditional intensity function of Weibull form is used for identifying the most appropriate among the models (simple, independent and linked stress release model) for the interpretation of the earthquake generation process. The appropriateness of the models was decided after evaluation via the Akaike information criterion. Despite the fact that the curves of the conditional intensity functions exhibit similar behavior, the use of the exponential-type conditional intensity function seems to fit better the data.

✉ Ourania Mangira
    omangira@geo.auth.gr

    Georgios Vasiliadis
    gvasil@math.auth.gr

    Eleftheria Papadimitriou
    ritsa@geo.auth.gr

[1] Geophysics Department, School of Geology, Aristotle University of Thessaloniki, 54124 Thessaloníki, Greece

[2] Department of Informatics Engineering, TEI of West Macedonia, 52100 Kastoria, Greece

## Introduction

The stress release model (SRM) was developed by Vere-Jones (1978) as a stochastic expansion of the elastic rebound theory (Reid 1910). This deterministic model assumes that the elastic stress is accumulated due to the long-term tectonic loading, and is released when it surpasses a certain level, i.e., the strength of the medium during the earthquake occurrence. The energy release should allow a certain time period to elapse until the re-accumulation of the energy and the genesis of a subsequent earthquake. Isham and Westcott (1979) first examined such a procedure, called a self-correcting point process, which automatically corrects a deviation from the mean number of points.

In a self-correcting process, the points display a repressive behavior, i.e., the occurrence of an event delays the occurrence of a subsequent event. It has been noticed very often though that shortly after a strong earthquake, a second one follows, with a long-term weak clustering characterizing all main shocks (Kagan and Jackson 1991). Gabrielov and Newman (1994) also support that a period of activation rather than a period of quiescence is observed after a main event and sometimes other earthquakes of comparable magnitude follow. This behavior could be explained with stress transfer between adjacent areas, and the idea is incorporated in the linked stress release model (LSRM) introduced by Liu et al. (1999). The interactions between different parts of an area are investigated in order to assess the impact an earthquake has on the seismicity of each part, and can provoke either damping or excitation of the earthquake activity in an adjacent subarea.

⏷ Springer

The stress release models (SRM) were widely applied during last decades for seismic hazard evaluation. The applications involve historical earthquakes from different regions worldwide, like China, Japan, Taiwan and New Zealand (e.g., Zheng and Vere-Jones 1994; Lu et al. 1999; Lu and Vere-Jones 2000; Bebbington and Harte 2003; Lu 2005; Imoto and Hurukawa 2006). In many of these studies, the main purpose was to identify statistically distinct regions by means of the AIC. Bebbington and Harte (2001) gave emphasis to the statistical behavior of the linked stress release model (LSRM) and suggested methods for checking the significance of the predicted interactions including residual process analysis and Monte Carlo simulation. Besides historical catalogs, synthetic earthquake catalogs were used for applying SRM (Liu et al. 1999; Lu and Vere-Jones 2001). The LSRM was also used to formulate a stochastic model for aftershocks (Borovkov and Bebbington 2003). More recently, information gains and entropy scores were proposed for scoring probability forecasts and trying to quantify the predictability of the stress release model (Bebbington 2005; Harte and Vere-Jones 2005). Comparisons were also made using Molchan's ν-τ diagram. A different approach is presented by Rotondi and Varini (2006, 2007) and Varini and Rotondi (2015) who analyzed stress release models from the Bayesian viewpoint, whereas Jiang et al. (2011) developed a new multidimensional SRM involving a coseismic stress transfer model.

Aiming to investigate the strong earthquake occurrence in two areas that frequently accommodate disastrous ($M \geq 6.0$) earthquakes, the Corinth Gulf and the Central Ionian Islands, the SRMs are applied. The earthquake interaction is examined between two subareas in which both study areas were subdivided. In the case of the Corinth Gulf, the area was subdivided into its western and eastern parts and in the case of the Central Ionian Islands, the two subareas consist of the Kefalonia (south part) and Lefkada (northern part) subareas. The application is performed by means of the conditional intensity function, and in particular of exponential type, like in the classical case, and of Weibull type. We will try to interpret and compare the results obtained from the two function types for determining which model is the most appropriate to explain the earthquake generation process.

## Formulation of the models

### Simple stress release model (SSRM)

In the simple stress release model (SSRM), the probability of an earthquake occurrence is determined by a quantity representing the stress level in an area (Vere-Jones and Deng 1988). The evolution of stress $X(t)$ as a function of time, could be written as

$$X(t) = X(0) + \rho t - S(t), \tag{1}$$

where $X(0)$ is the initial stress value, $\rho$ is the loading rate and $S(t)$ is the accumulated stress release from earthquakes within the area over the period $(0, t)$, i.e.,

$$S(t) = \sum_{t_i < t} S_i, \tag{2}$$

where $t_i$, $S_i$ are the origin time and the stress release, respectively, associated with the $i$ th earthquake.

The amount of stress released during an earthquake can be approximated by empirical relations. Bufe and Varnes (1993) suggest that a measure of the total energy released is the cumulative Benioff strain, i.e., $S(t) = \sum_{i=1}^{N(t)} E_i^{1/2}$, where $E_i$ is the seismic energy of the $i$ th earthquake and $N(t)$ stands for the number of earthquakes till time $t$. The seismic energy released is given by the relation $E = 10^{3/2M} + \text{const}$ (Kanamori and Anderson 1975). Then

$$S = 10^{0.75(M - M_{\text{th}})}, \tag{3}$$

where $M$ is the earthquake magnitude and $M_{\text{th}}$ the smallest magnitude appeared in the dataset.

The stochastic behavior of the model is characterized by the conditional intensity function $\lambda^*(t)$ (Daley and Vere-Jones 2003), which is assumed to have the exponential form

$$\begin{aligned} \lambda^*(t) = \Psi(X(t) &= \exp\{\mu + v[X(0) + \rho t - S(t)]\} \\ &= \exp\{a + v[\rho t - S(t)]\} \\ &= \exp\{a + b[t - cS(t)]\}, \end{aligned} \tag{4}$$

where $a$, $b$, $c$ are the parameters to be fitted. The estimation is performed numerically by maximizing the log-likelihood function

$$\log L = \sum_{i=1}^{N(T)} \log \lambda^*(t) - \int_0^T \lambda^*(u) \, du, \tag{5}$$

where $(0, T)$ is the observational interval and $N(T)$ is the total number of events in $(0, T)$.

A Weibull-type conditional intensity function (c.i.f.) might be additionally applied, because it is among the most commonly used ones in survival analysis and quite flexible since it is related to a number of other probability distributions. The following form for the conditional intensity function is assumed (Votsi et al. 2011)

$$\lambda^*(t) = \lambda \gamma X(t)^{\gamma - 1} = \lambda \gamma (X(0) + \rho t - S(t))^{\gamma - 1} \tag{6}$$

The parameters to be estimated are $\lambda$, $\gamma$, $X(0)$, $\rho$.

## Linked stress release model (LSRM)

The incorporation of the interactions between different subareas, which is not taken into account in the formulation of the SSRM, leads to the linked stress release model (LSRM). The stress evolution in the $i$ subarea is now written

$$\lambda_i^*(t) = \exp\left\{a_i + b_i\left[t - \sum_j c_{ij}S(t,j)\right]\right\}, \tag{7}$$

where $S(t, j)$ stands for the accumulated stress release in the $j$ subarea over the period $(0, t)$ and $\theta_{ij}$ measures the fixed ratio of stress release, which is transferred from the $j$ to the $i$ subarea. It is plausible to set $\theta_{ii} = 1$, since it is assumed that at least a significant amount of the accumulated energy is released. Positive and negative values of $\theta_{ij}$ indicate damping and excitation, respectively.

In the original formulation of the LSRM it is assumed for each subarea a c.i.f. of the form

$$\lambda_i^*(t) = \Psi(X_i(t)) = \exp\left\{a_i + v_i\left[\rho_i t - \sum_j \theta_{ij}S(t,j)\right]\right\}, \tag{8}$$

where $\alpha_i\ (=\mu_i + v_i\, X_i(0))$, $v_i$, $\rho_i$ and $\theta_{ij}$ are the parameters to be fitted. Liu et al. (1998) achieve a more convenient parameterization by setting $b_i = v_i\rho_i$ and $c_{ij} = \theta_{ij}/\rho_i$.

$$\lambda_i^*(t) = \exp\left\{a_i + b_i\left[t - \sum_j c_{ij}S(t,j)\right]\right\}, \tag{9}$$

where $a_i$, $b_i$, $c_{ij}$ are the parameters to be fitted for each subarea $i$.

For the parameters to be estimated some restrictions exist that should be taken into account. The parameters $b_i = v_i\rho_i$ and $c_{ii} = 1/\rho_i$ should be positive, since the loading rate $\rho_i$ and the sensitivity to stress change, $v_i$, take (only) positive values. On the contrary, $c_{12}$ and $c_{21}$ could take either positive or negative values, since they indicate the style of interactions between adjacent subareas, i.e., if they are inhibitory or excitatory.

Supposing that a Weibull-type conditional intensity function fits better the data, for each subarea $i$ we assume that

$$\begin{aligned}\lambda_i^*(t) &= \lambda_i\gamma_i X_i(t)^{\gamma_i - 1} \\ &= \lambda_i\gamma_i\left(X_i(0) + \rho_i t - \sum_j \theta_{ij}S(t,j)\right)^{\gamma_i - 1}\end{aligned} \tag{10}$$

The parameters to be estimated are $\lambda_i$, $\gamma_i$, $X_i(0)$, $\rho_i$ and $\theta_{ij}$, where $\lambda_i > 0$ and $\gamma_i > 0$. The shape parameter $\gamma$ determines the behavior of the conditional intensity function. A value of $\gamma$ lower than 1 implies that the failure rate

decreases over time, whereas if $\gamma > 1$ there is an increasing hazard over time. The failure rate is constant over time when the shape parameter takes the value $\gamma = 1$, and in that case the Weibull distribution turns out to an exponential one. We impose the restriction of $\gamma \geq 1$ since earthquakes are more likely to occur as time advances.

It should be noticed that, for the number of parameters to be constrained, a large data sample is required. Since we assume that the occurrence of earthquakes reduces the probability of immediately subsequent events, we are only interested in the strong events which are of primary practical concern.

## Study areas and data

Both study areas were extensively investigated since they have accommodated several destructive earthquakes that occurred both in historical and instrumental era. The Corinth rift (Fig. 1) consists of one of the most rapidly extending areas worldwide (Armijo et al. 1996). The high level of seismicity is testified by the historical as well as the instrumental records, with the maximum magnitude observed or ever reported hardly >6.8 (Papazachos and Papazachou 2003), a fact that probably reflects the lack of continuity of fault segments (Jackson and White 1989). One observation worth to be mentioned here is the sequence of three earthquakes with $M \geq 6.3$ that occurred in 1981 in ten days in the eastern part of the Corinth Gulf (Console et al. 2013). The SSRM was applied in the western part of the Corinth Gulf by Rotondi and Varini (2006) with a smaller dataset of 20 earthquakes including events with $M \geq 5.0$ since 1945 and after performing Bayesian analysis.

The central Ionian Islands area (Fig. 2), which includes Lefkada and Kefalonia Islands, consists of one of the most
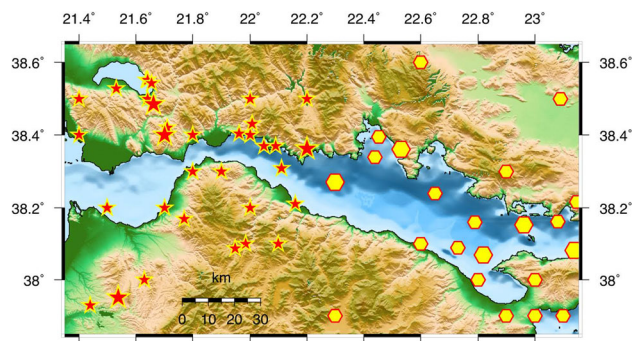


**Fig. 1** Seismicity map for the Corinth Gulf showing earthquakes with magnitude $M \geq 5.2$ that occurred in the area since 1911. The events occurred in the western part are represented with *red stars*, whereas the ones occurred in the eastern part are represented with *yellow hexagons*. Their size is proportional to the earthquake's magnitude
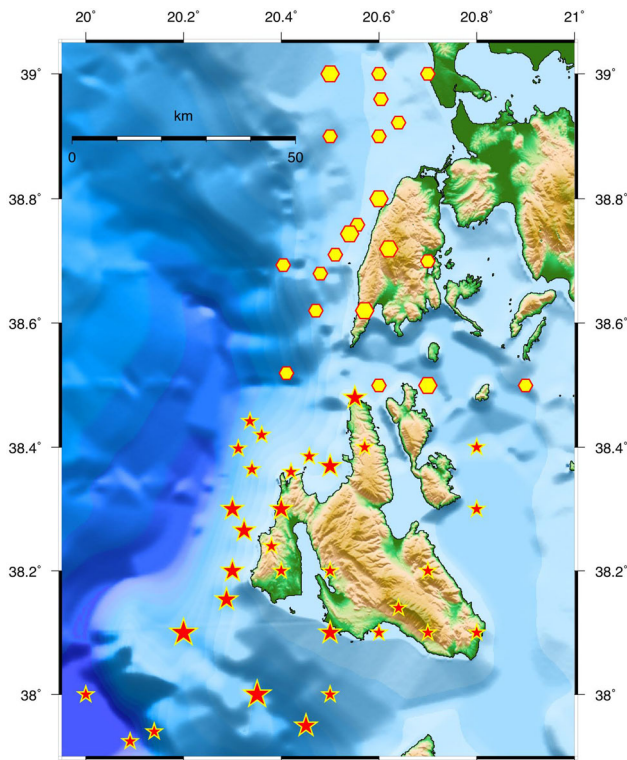
**Fig. 2** Seismicity map for the Central Ionian Islands showing earthquakes with magnitude $M \geq 5.2$ that occurred in the area since 1911. The events occurred in the subarea of Kefalonia are represented with *red stars*, whereas the ones occurred in the subarea of Lefkada are represented with *yellow hexagons*. Their size is proportional to the earthquake magnitude

seismically active areas in the broader Aegean region, a fact that is clearly showed by the high seismic moment rate ($>10^{25}$ dyn cm year$^{-1}$) (Papazachos et al. 1997). The Kefalonia Transform Fault Zone (KTFZ) was recognized as responsible for the high seismicity levels of in the region, connecting the continental collision to the north with the oceanic subduction to the south (Scordilis et al. 1985). Seismicity is mainly observed in the sea area along the west shoreline and offshore of the two islands.

Lefkada Island has suffered many times from earthquakes occurring in the nearby Kefalonia Island, a fact that suggests possible coupling between the Lefkada and Kefalonia faults (Papadimitriou 2002). Therefore, it is particularly interesting to examine the interactions between earthquakes occurring in each subarea via stress release models. Votsi et al. (2011) were the first to apply stress release models to this area. Two different complete datasets were used in their study, one comprising earthquakes with $M \geq 6.0$ in the period 1862–2008 for the application of the SSRM and one comprising earthquakes with magnitudes $M \geq 5.2$ that occurred from 1911 to 2008, for the application of the LSRM. In the second case, the magnitude threshold is lower since more data are needed when

applying the LSRM due to the larger number of parameters. The division of the subareas of Kefalonia and Lefkada is slightly different than the one chosen in this study, as well as the dataset used (period selected, magnitude cut-off). In this paper, a so-called Weibull model was also proposed, suggesting a conditional intensity function of Weibull form in the case of the SSRM, i.e., taking the entire study area as one, which was served as a basic idea in our study.

For both study areas, the magnitude threshold was set as low as $M_{th} = 5.2$ from January 1st, 1911 to December 31st, 2015 to obtain the largest and longest possible complete earthquake catalog. The data used are taken from the catalog compiled in the Geophysics Department of Aristotle University of Thessaloniki (Aristotle University of Thessaloniki Seismological Network 1981). In the case of the Corinth Gulf, the catalog comprises 61 events, 36 of which occurred in the western and 25 in the eastern part. In the case of the Central Ionian Islands, 74 events in total were used, with the most seismically active subarea of Kefalonia comprising 41 events, and the Lefkada subarea including 33.

## Application of the models

As mentioned above, the estimation of the parameters is performed by maximizing the log-likelihood function. The optimization algorithm is usually executed many times starting from different initial values of the parameters randomly drawn from the parameter space. The estimated parameters are those corresponding to the maximum among the derived maximum log-likelihood values. To achieve successful convergence as well as minimize randomness, the initial points were not randomly selected, but after scanning numerically the parameter space and taking into account the restrictions of the models. A Newton-type algorithm (specifically the BFGS method) was then performed, where the initial parameters are those found by the above search.

Particular caution should be given to the application of the Weibull-type LSRM, since the form of the conditional intensity function may create problems when estimating the model parameters. Negative values for the stress function $X_i(t)$ lead to negative values for the conditional intensity function, which is unacceptable. The optimization algorithm was created for exclusion of the problematic points. Constraints are set so that the quantity which is interpreted as stress in each subarea, $X_i(t)$, takes only positive values. The final points therefore do not create any problem in the optimization process.

The evaluation of the models could be performed by means of the Akaike information criterion (AIC) which is used as a measure of distinction between the two

competing models (Akaike 1974). The AIC represents a method of penalizing additional parameters in a model to avoid over-fitting.

## Application of the SRMs to the Corinth Gulf

### LSRM: exponential-type conditional intensity function

The LSRM is applied for investigating coupling between two subareas in the Corinth Gulf, i.e., the western and eastern part, where the conditional intensity function is of exponential type (9). The parameters are derived through the MLE method. Additional constraints are put such that the parameters $b_1$, $b_2$, $c_{11}$ and $c_{22}$ take only positive values. In order to estimate constrained parameters with the MLE method, each positive parameter is re-parametrized as an exponential function of a parameter lying on the real line. The estimated parameters are presented in Table 1, along with the corresponding standard errors and the 90% confidence intervals. The maximum value of the log-likelihood function is $-132.508$.

Both transfer parameters $c_{ij}$ are positive, which indicates inhibitory behavior, suggesting that earthquake occurrence in one subarea reduces the activity in the second one. Figure 3 shows the conditional intensity function for the western (Fig. 3a) and eastern (Fig. 3b) part, respectively. In the same figures, the earthquake magnitudes versus time are plotted for the same dataset in order to see the relation between the events and the c.i.f.. Particularly we may observe that in the eastern part (Fig. 3b) the stress drops appear to be larger when an event occurs in the western part rather than in the eastern subarea itself, which is evidenced by the large value of the parameter $c_{21}$ showing correlation between the two subareas. The loading rate of the eastern part—and not the triggering from the western part—seems to designate the earthquake occurrence.

### LSRM: Weibull-type conditional intensity function

The LSRM with Weibull-type conditional intensity function given in (10) is applied in an effort to find a better fitting to the data of the Corinth Gulf. Using a BFGS optimization algorithm, the maximum value of the log–likelihood function is found to be $-133.9383$ under appropriate constraints, meaning that the parameters $\lambda_i$, $\gamma_i$, $\rho_i$ are positive alike the stress function $Xi(t)$. The estimate of gamma does not turn out to be >1, $\gamma_i > 1$, by simply setting the restriction $\gamma_i > 0$. The restriction of $\gamma_i > 1$ is necessary therefore for the failure rate of the Weibull-type LSRM being increased.

Table 2 shows the estimated parameters, the standard errors and the 90% confidence intervals for the LSRM applied in the same dataset. The results are in accordance with the ones using an exponential-type conditional intensity function. The parameters $\theta_{12}$ and $\theta_{21}$ are positive, indicating damping of each subarea due to earthquakes occurring in the adjacent subarea. We notice though that the confidence interval for both transfer parameters, $\theta_{12}$ and $\theta_{21}$, contain positive as well as negative values indicating that the influence of the one part to the other is not robust in the sense that the parameter could also take the value 0 since it is included in the confidence interval. This is partly in accordance with the case using the exponential-type conditional intensity function, where both transfer parameters were found positive and the parameter $\theta_{21}$ was strictly positive. The conditional intensity functions for both subareas are shown in Fig. 4.

The evaluation of the models is performed by means of the Akaike information criterion (AIC), as mentioned before. The value of the log-likelihood function is greater when using an exponential-type c.i.f., and the value of the AIC is smaller since in this case the model parameters are 8, less than in the Weibull-type c.i.f. case by two. We can

**Table 1** LSRM's estimated parameters, standard errors and confidence intervals when using an exponential-type conditional intensity function

| Parameter | Estimate | | Standard error | | 90% Confidence interval | |
|---|---|---|---|---|---|---|
| | Corinth Gulf | Central Ionian Islands | Corinth Gulf | Central Ionian Islands | Corinth Gulf | Central Ionian Islands |
| $a_1$ | $-1.993$ | 0.250 | 0.449 | 0.420 | $(-2.731, -1.255)$ | $(-0.441, 0.942)$ |
| $a_2$ | $-1.601$ | 0.470 | 0.607 | 0.387 | $(-2.599, -0.602)$ | $(-0.166, 1.107)$ |
| $b_1$ | 0.040 | 0.027 | 0.036 | 0.754 | $(0.022, 0.072)$ | $(0.008, 0.093)$ |
| $b_2$ | 0.046 | 0.040 | 0.522 | 0.469 | $(0.019, 0.108)$ | $(0.018, 0.087)$ |
| $c_{11}$ | 0.681 | 0.117 | 0.861 | 2.517 | $(0.165, 2.802)$ | $(0.002, 7.341)$ |
| $c_{12}$ | 0.360 | 1.406 | 0.352 | 0.857 | $(-0.219, 0.940)$ | $(-0.003, 2.816)$ |
| $c_{21}$ | 1.698 | 0.241 | 0.929 | 0.223 | $(0.169, 3.227)$ | $(-0.127, 0.608)$ |
| $c_{22}$ | 0.171 | 1.147 | 2.532 | 0.491 | $(0.003, 11.025)$ | $(0.511, 2.573)$ |

**Fig. 3** The exponential-type conditional intensity function versus time for each subarea of the Corinth Gulf, fitted to the catalog of earthquakes with $M \geq 5.2$ that occurred since 1911. **a** Western part. **b** Eastern part
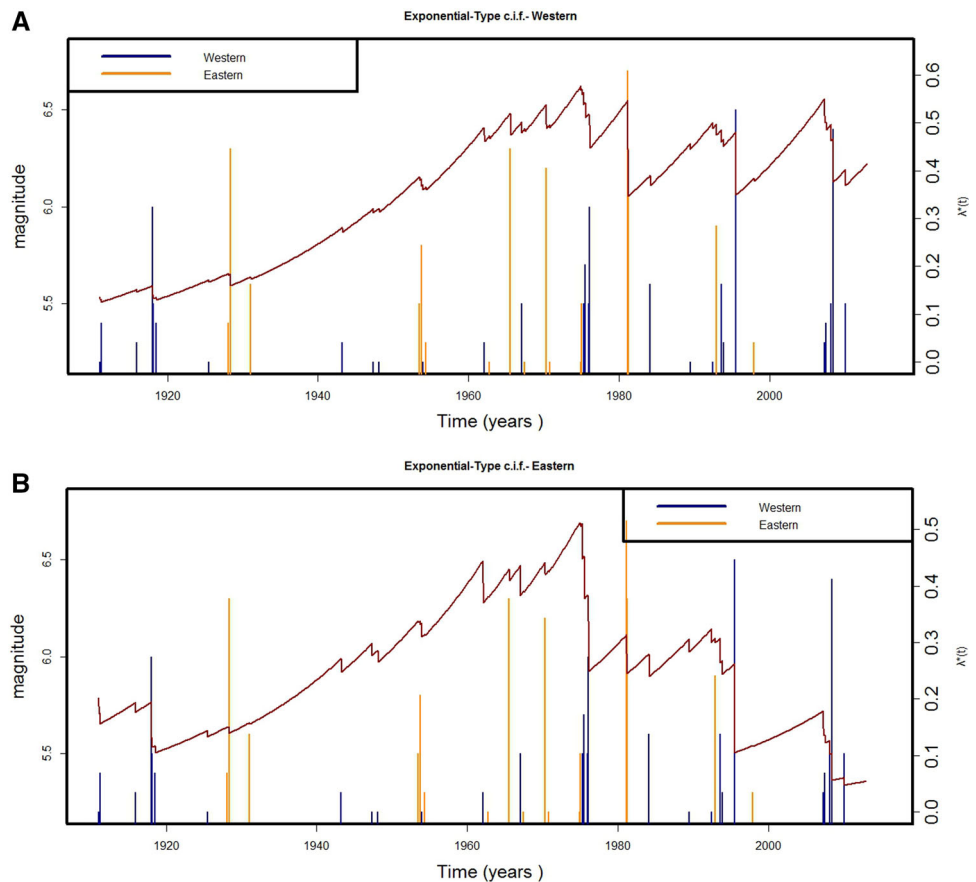


**Table 2** LSRM' estimated parameters, standard errors and confidence intervals when using a Weibull-type conditional intensity function

| Parameter | Estimate | | Standard error | | 90% Confidence interval | |
|---|---|---|---|---|---|---|
| | Corinth Gulf | Central Ionian Islands | Corinth Gulf | Central Ionian Islands | Corinth Gulf | Central Ionian Islands |
| $\lambda_1$ | 0.125 | 0.012 | 0.647 | 4.590 | (0.043, 0.362) | $(6.2 \times 10^{-6}, 22.505)$ |
| $\lambda_2$ | 0.003 | 0.0003 | 2.391 | 7.403 | $(6.6 \times 10^{-5}, 0.173)$ | $(1.68 \times 10^{-9}, 59.265)$ |
| $\gamma_1$ | 1.234 | 1.717 | 0.369 | 1.304 | (1.128, 1.429) | (1.084, 7.128) |
| $\gamma_2$ | 1.950 | 2.354 | 0.470 | 1.005 | (1.439, 3.057) | (1.259, 8.069) |
| $X_1(0)$ | 37.826 | 112.107 | 4.270 | 12.185 | (30.801, 44.850) | (176.554, 180.507) |
| $X_2(0)$ | 68.572 | 178.531 | 8.052 | 1.202 | (55.327, 81.817) | (62.58, 94.60) |
| $\rho_1$ | 2.056 | 2.045 | 0.332 | 0.590 | (1.191, 3.551) | (0.748, 5.398) |
| $\rho_2$ | 1.434 | 1.430 | 0.351 | 0.815 | (0.805, 2.555) | (0.374, 5.467) |
| $\theta_{12}$ | 1.500 | 0.769 | 1.934 | 1.265 | (−1.681, 4.681) | (−1.311, 2.850) |
| $\theta_{21}$ | 1.800 | 0.957 | 1.527 | 0.841 | (−0.713, 4.312) | (−0.426, 2.341) |

thus argue that we can avoid over-fitting since the use of the two extra parameters is not necessary finally.

*Independent SRM: exponential-type conditional intensity function*

As mentioned in the previous section, by checking the interval estimation of the transfer parameters $c_{ij}$, we may see that only the parameter $c_{21}$ is positive, meaning that one-way interaction is established. We cannot argue about the way earthquakes occurring in the eastern part influence the western part. Since 0 is included in the interval estimation of $c_{12}$, we applied the SRM separately in the western part of the Corinth Gulf, i.e., under the assumption that earthquakes occurring in the eastern part don't affect the ones of the western part. The parameters shown in Table 3 are estimated through the MLE method and the conditional intensity function versus time is plotted in Fig. 5.

**Fig. 4** The Weibull-type conditional intensity function versus time for each subarea of the Corinth Gulf, fitted to the catalog of earthquakes with $M \geq 5.2$ that occurred since 1911. **a** Western part. **b** Eastern part
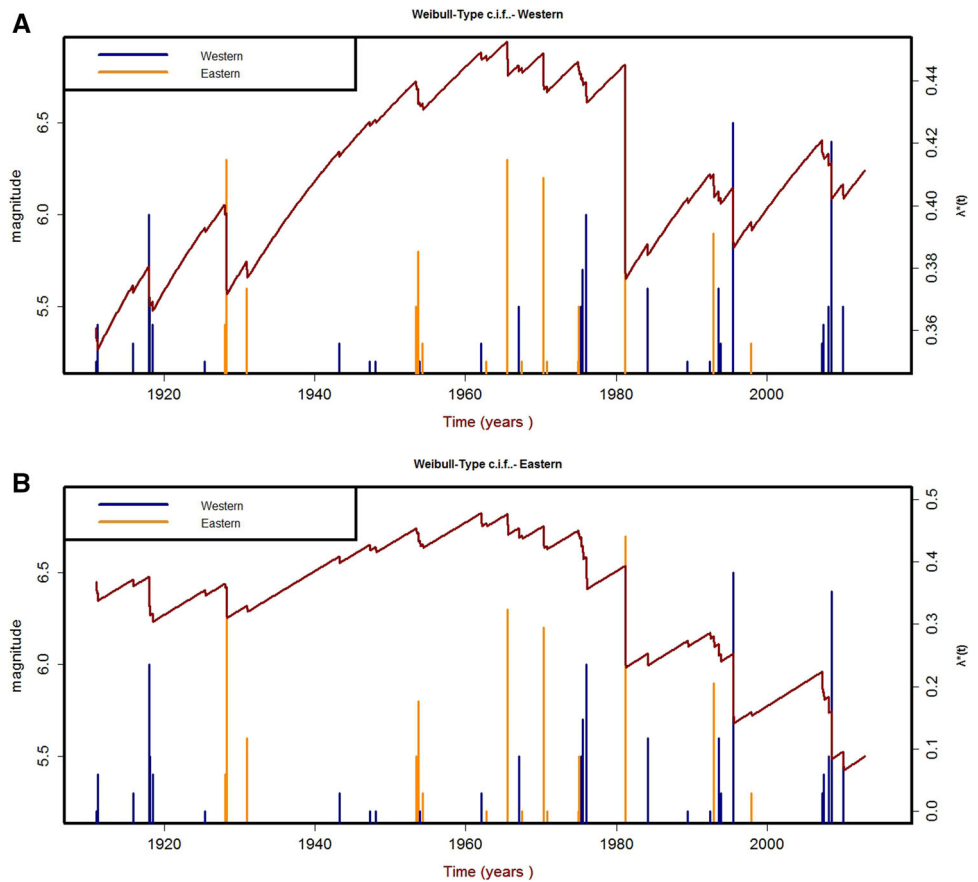


**Table 3** Estimated parameters, standard errors and confidence intervals for the ISRM (western part of the Corinth Gulf) and the SSRM when using an exponential-type conditional intensity function

| Parameter | Estimate | | Standard error | | 90% Confidence interval | |
|---|---|---|---|---|---|---|
| | ISRM (western part) | SSRM | ISRM (western part) | SSRM | ISRM (western part) | SSRM |
| $a$ | −1.708 | −0.865 | 0.420 | 0.326 | (−2.399, −1.018) | (−1.403, −0.328) |
| $b$ | 0.026 | 0.014 | 0.016 | 1082 | (0.0001, 0.052) | (0.002, 0.086) |
| $c$ | 1.089 | 0.468 | 0.492 | 0.573 | (0.280, 1.898) | (0.182, 1.201) |

**Fig. 5** The exponential-type conditional intensity function versus time when applying the ISRM to the western part of the Corinth Gulf
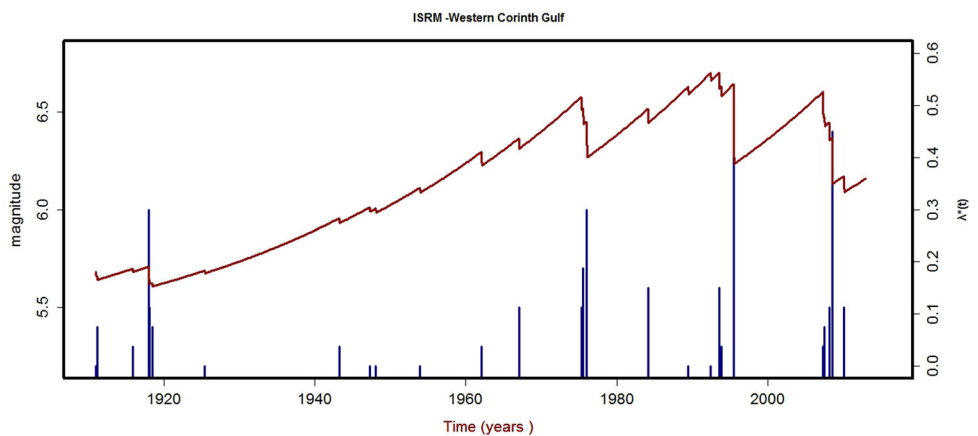
**Table 4** Estimated parameters, standard errors and confidence intervals for the ISRM and SSRM in the Corinth Gulf when using a Weibull-type conditional intensity function

| Parameter | Estimate | | | Standard error | | | 90% Confidence interval | | |
|---|---|---|---|---|---|---|---|---|---|
| | ISRM (western part) | ISRM (eastern part) | SSRM | ISRM (western part) | ISRM (eastern part) | SSRM | ISRM (western part) | ISRM (eastern part) | SSRM |
| $\lambda$ | 0.023 | 0.002 | 0.009 | 4.813 | 7.761 | 3.812 | $(8.3 \times 10^{-6}, 63.254)$ | $(4.7 \times 10^{-9}, 577.4)$ | $(1.7 \times 10^{-5}, 4.618)$ |
| $\gamma$ | 1.530 | 2.071 | 1.776 | 0.654 | 0.890 | 0.415 | (0.522, 4.489) | (0.479, 8.958) | (0.898, 3.512) |
| $X(0)$ | 50.296 | 29.698 | 75.041 | 5.027 | 7.293 | 10.214 | (42.027, 58.565) | (17.770, 41.696) | (58.239, 91.843) |
| $\rho$ | 1.050 | 1.127 | 1.863 | 0.980 | 0.634 | 0.398 | (0.210, 5.263) | (0.397, 3.199) | (0.968, 3.588) |

**Fig. 6** The Weibulll-type conditional intensity function versus time when applying the ISRM to the **a** western part, **b** eastern part of the Corinth Gulf
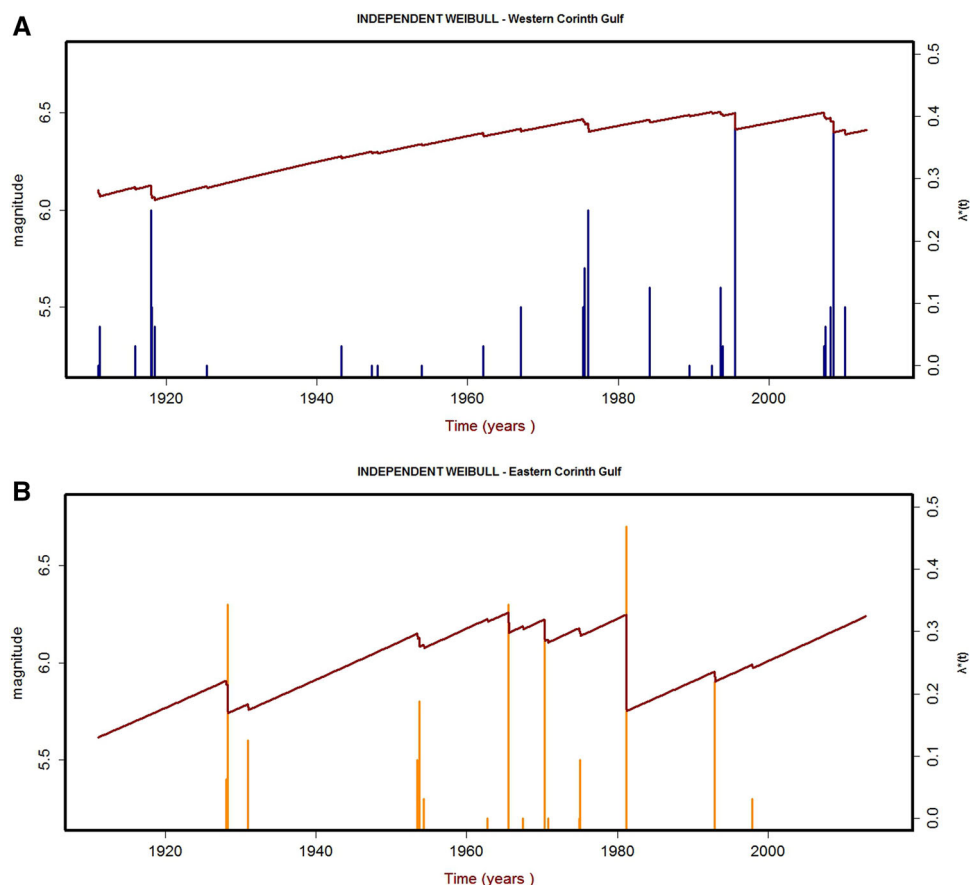


### Independent SRM: Weibull-type conditional intensity function

The interval estimation of both $c_{12}$ and $c_{21}$ transfer parameters in the case of the Weibull-type c.i.f., contain the value 0. It is, therefore, plausible to apply the independent stress release model (ISRM), i.e., apply the SSRM in each subarea separately. The estimated parameters for both parts of the Corinth Gulf are shown in Table 4, along with the corresponding standard errors and the 90% confidence intervals, and the conditional intensity functions are shown in Fig. 6a, b, respectively.

### SSRM: exponential-type conditional intensity function

A more profound and complete investigation of the best model fitting the dataset requires the application of the SSRM. In the SSRM, no spatial interactions of earthquake
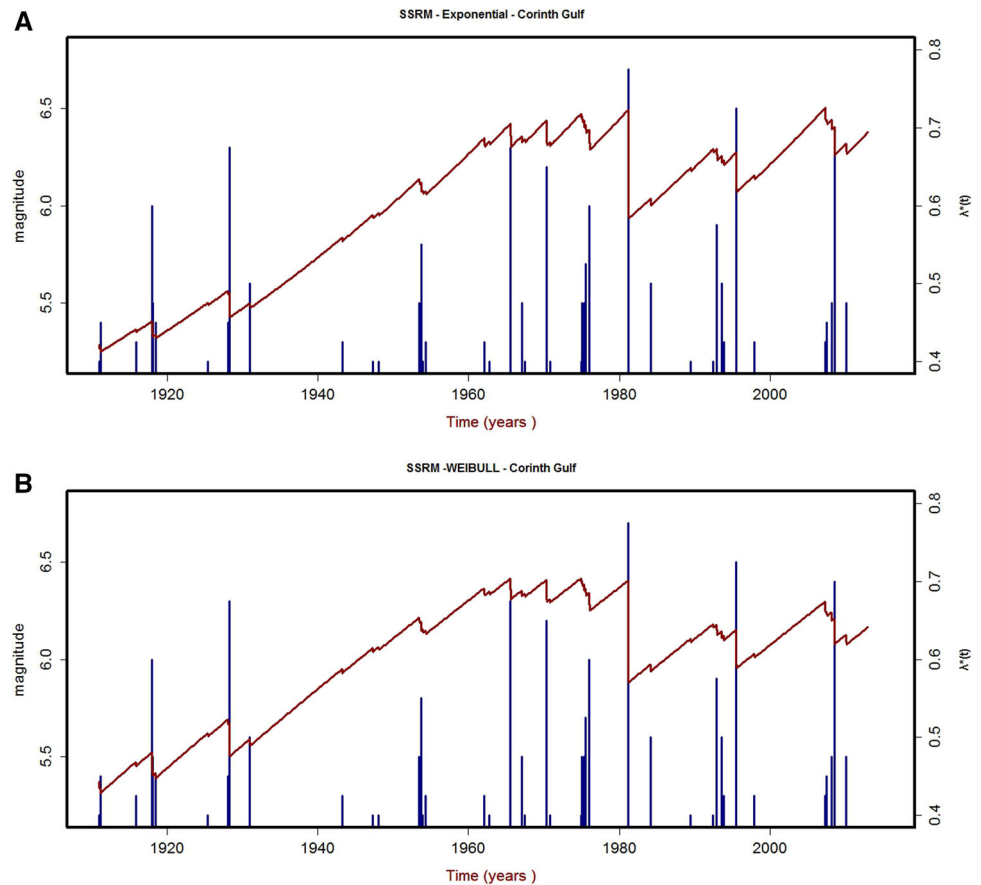
occurrence through stress transfer are considered between different parts and for this reason the study area is considered as one entity. Thus, a c.i.f. of exponential-type (4) is used, resulting in the parameters presented in Table 3 and the corresponding plot in Fig. 7a.

### SSRM: Weibull-type conditional intensity function

The alternative form (5) suggesting a Weibull-type c.i.f. is also used. The four estimated parameters (Table 4) are derived through the MLE method and particularly by means of the BFGS optimization algorithm with constraints not only for the parameters to be positive but also for affirming that X(t) takes only positive values. The conditional intensity function versus time is plotted in Fig. 7b, where the two plots of the simple stress release models are similar. Under this assumption the two models are equivalent. Based on the information criteria, the exponential-type c.i.f. should be preferred (approximately difference of 2 in AIC). Based exclusively on the AIC, we could select the SSRM versus the LSRM, but since we are interested in the interactions between the subareas and at least one confidence interval takes only positive values we can still claim that the LSRM could interpret the seismicity of the area.

### Application of the LSRM to the area of Central Ionian Islands

#### LSRM: exponential-type conditional intensity function

As in the case of the Corinth Gulf, the maximum likelihood estimation method is used in the application of the LSRM to the Central Ionian Islands area in order to estimate the model parameters. Constraints are put such that the confidence intervals for the parameters $b_i$ and $c_{ii}$ contain only positive values. The model parameters as well as the standard errors and the 90% confidence intervals are shown in Table 1. The log-likelihood function attains the maximum value of $-143.166$.

In Fig. 8 the conditional intensity functions versus time are plotted for both subareas of Kefalonia and Lefkada, along with the temporal distribution of the earthquake magnitudes. We observe that the curves display high values at the beginning of the study period followed by a sudden decrease. This is due to the positive values of $a_1$ and $a_2$, since the conditional intensity functions at time $t = 0$ take the value $\lambda^* (0) = \exp \{a\}$. Besides, due to the lack of preceding information the first period results cannot be unambiguously considered as reliable and might not be taken into account. Based on the estimated parameters we

**Fig. 8** The exponential-type conditional intensity function versus time for each subarea of the Central Ionian Islands, fitted to the catalog of earthquakes with $M \geq 5.2$ that occurred since 1911. **a** Kefalonia. **b** Lefkada
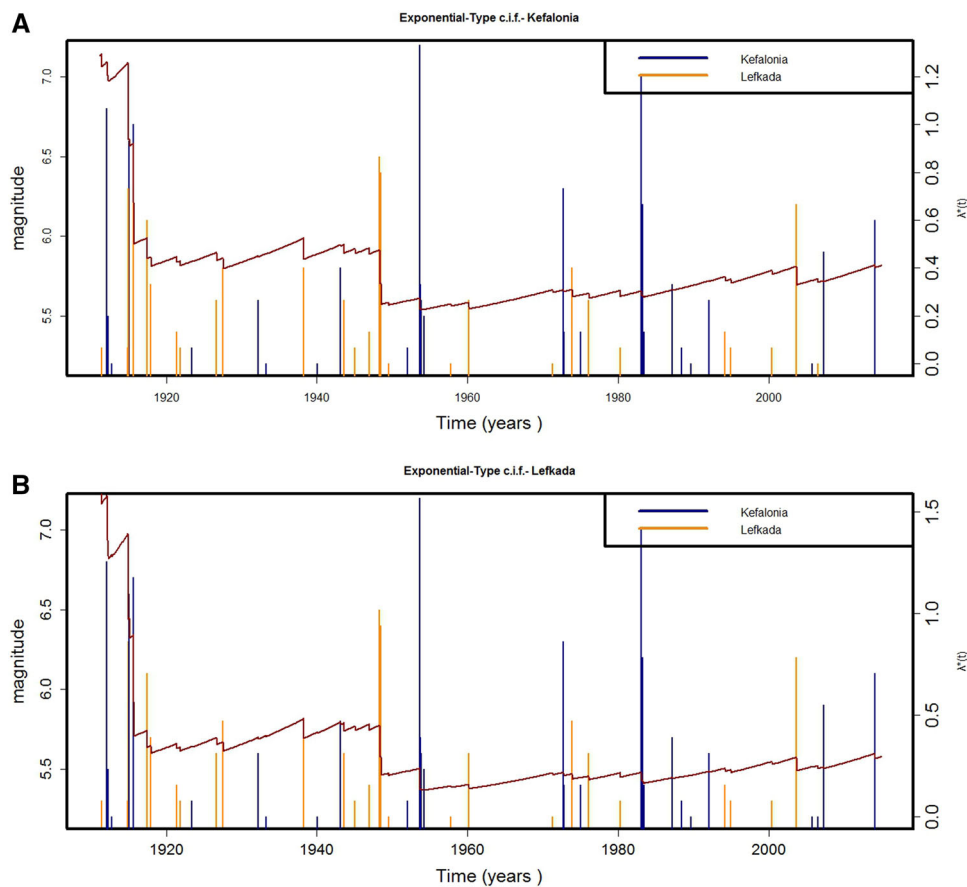


can interpret the behavior of the conditional intensity functions for the two subareas. Both transfer parameters are positive, implying inhibitory behavior. The parameter $c_{21}$ was found to be positive; the 90% confidence interval though contains also negative values meaning that the interactions are not robust in the sense that the parameter could also take the value 0 since it is included in the confidence interval.

We can also see that the application of the LSRM reveals that the loading rate $\rho_1 = 1/c_{11}$ of the subarea of Kefalonia is higher than the one of Lefkada, which is in accordance with the tectonic loading in the two subareas quantified by seismological and geodetic observations. In any case, there is close resemblance between the two curves indicating the strong relationship between earthquakes occurring in the two subareas.

### LSRM: Weibull-type conditional intensity function

The LSRM is applied to the central Ionian Islands under the assumption of the Weibull-type conditional intensity function. The Newton-type optimization algorithm led to the parameters values presented in Table 2. The maximum value of the log-likelihood function is computed and found equal to $-145.4507$. Both transfer parameters $\theta_{12}$ and $\theta_{21}$

are estimated and found to be positive. The 90% confidence intervals though are not strictly positive, indicating that the style of interactions between the two subareas based on the LSRM cannot be unambiguously certified. The two curves of the conditional intensity functions (Fig. 9) display similar behavior. The loading rate, $\rho_1$, is higher in Kefalonia, which agrees with the more frequent and larger magnitude here than in Lefkada.

The two competing models are assessed via the AIC. The estimated maximum log-likelihood is slightly greater in the classical LSRM than in the Weibull-type LSRM and additionally, the fact that AIC penalizes the extra parameters, the "classical" model of the exponential form is proved to be better. Therefore, although the proposed model of the Weibull form seems to interpret the behavior and the interactions between the two subareas in a similar way with the exponential form, the two extra parameters do not add enough information and, therefore, the new form against the classical one is selected.

### ISRM: exponential-type conditional intensity function

The interval estimation presented in Table 4 shows that stress transfer—and particularly damping—is established from the subarea of Lefkada to the subarea of Kefalonia,

**Fig. 9** The Weibull-type conditional intensity function versus time for each subarea of the Central Ionian Islands, fitted to the catalog of earthquakes with $M \geq 5.2$ that occurred since 1911
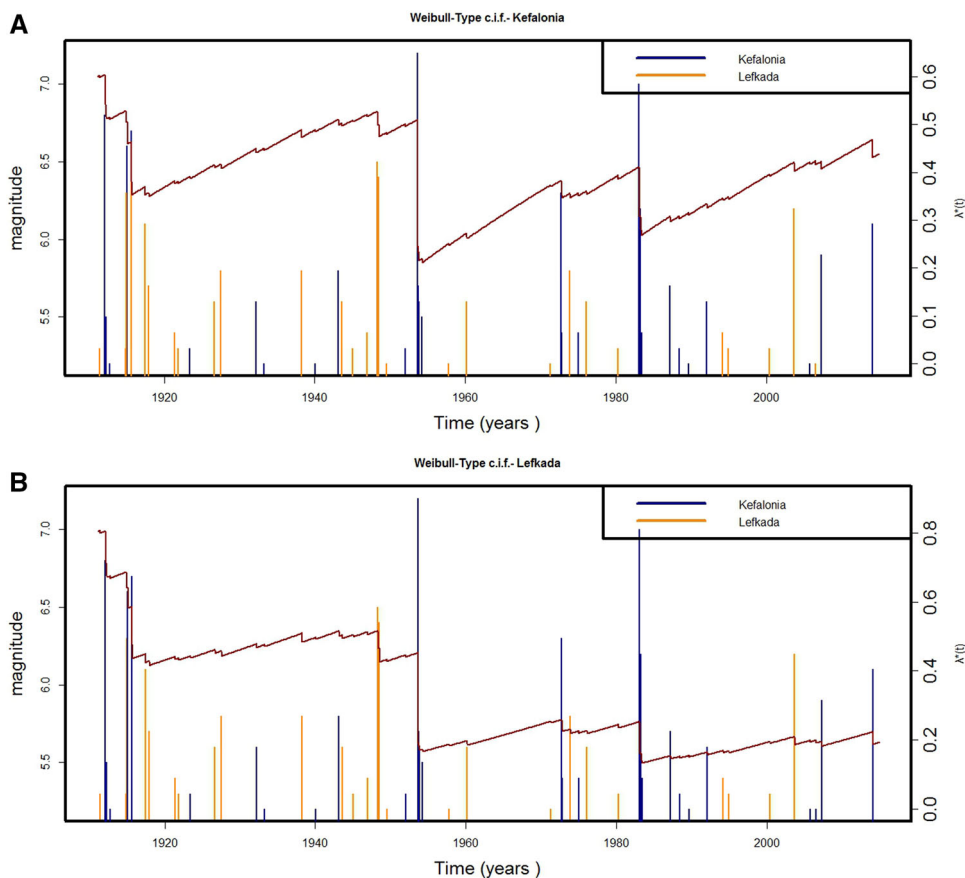


**Table 5** Estimated parameters, standard errors and confidence intervals for the ISRM (Lefkada) and the SSRM when using an exponential-type conditional intensity function

| Parameter | Estimate | | Standard error | | 90% Confidence interval | |
|---|---|---|---|---|---|---|
| | ISRM (Lef.) | SSRM | ISRM (Lef.) | SSRM | ISRM (Lef.) | SSRM |
| $a$ | 0.172 | 0.654 | 0.415 | 0.317 | (−0.511, 0.855) | (0.133, 1.174) |
| $b$ | 0.013 | 0.018 | 1.343 | 0.918 | (0.001, 0.115) | (0.004, 0.082) |
| $c$ | 2.721 | 0.654 | 0.836 | 0.402 | (0.688, 10.762) | (0.337, 1.267) |

**Fig. 10** The exponential-type conditional intensity function versus time when applying the ISRM to the subarea of Lefkada
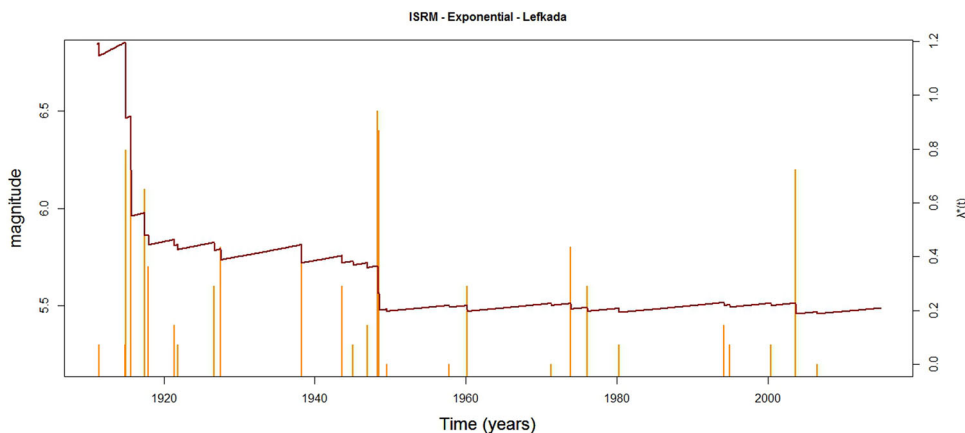
**Fig. 11** The Weibull-type conditional intensity function versus time when applying the ISRM to the subarea of **a** Kefalonia, **b** Lefkada
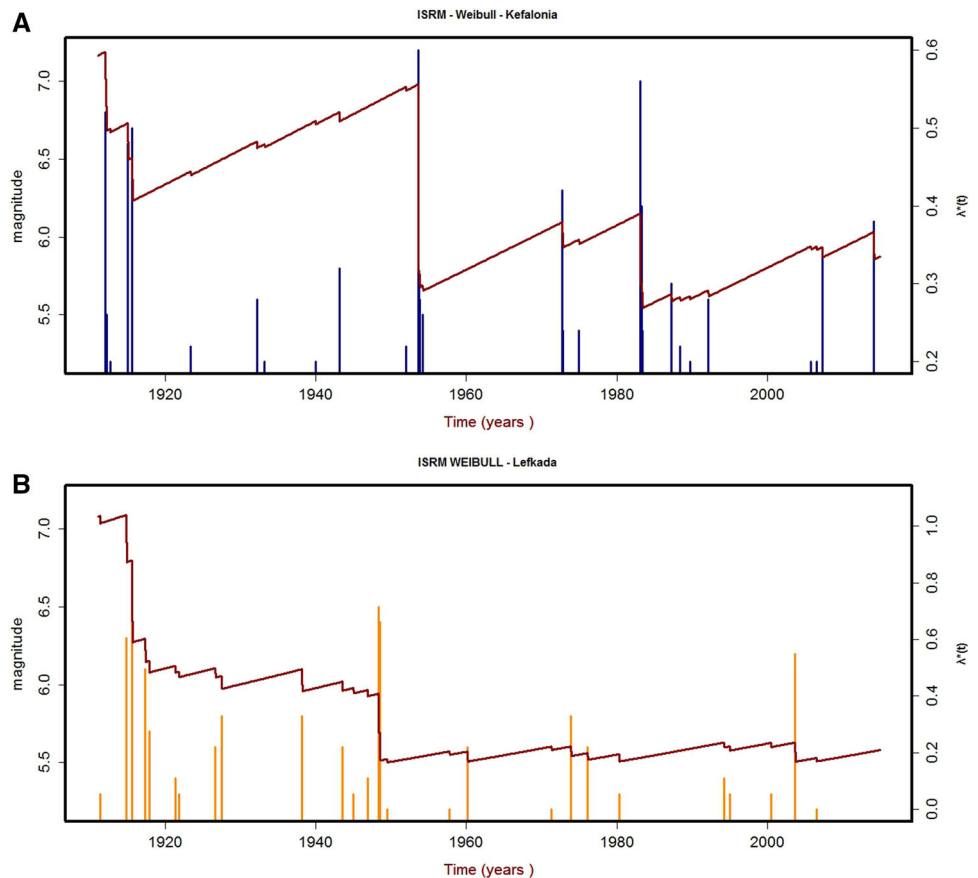


**Table 6** Estimated parameters, standard errors and confidence intervals for the ISRM and SSRM in central Ionian Islands when using a Weibull-type conditional intensity function

| Parameter | Estimate | | | Standard error | | | 90% Confidence interval | | |
|---|---|---|---|---|---|---|---|---|---|
| | ISRM (Kef.) | ISRM (Lef.) | SSRM | ISRM (Kef.) | ISRM (Lef.) | SSRM | ISRM (Kef.) | ISRM (Lef.) | SSRM |
| $\lambda$ | 0.0009 | 0.0005 | 0.005 | 7.340 | 6.367 | 3.307 | $(5.3 \times 10^{-9}$, 162.23) | $(1.4 \times 10^{-8}$, 16.941) | $(2.2 \times 10^{-5}$, 1.190) |
| $\gamma$ | 2.131 | 2.564 | 1.985 | 0.646 | 0.521 | 0.317 | (0.737, 6.164) | (1.088, 6.040) | (1.178, 3.345) |
| $X(0)$ | 155.051 | 74.063 | 152.116 | 6.563 | 25.856 | 9.506 | (144.255, 165.848) | (31.530, 116.595) | (136.48, 167.75) |
| $\rho$ | 1.178 | 0.399 | 1.759 | 0.474 | 0.521 | 0.190 | (0.541, 2.568) | (0.169, 0.940) | (1.287, 2.404) |

while the reverse interaction cannot be fully justified. Therefore, the seismicity of the Lefkada subarea can be modeled by means of the ISRM. The estimated parameters are presented in Table 5 and the corresponding c.i.f. is shown in Fig. 10.

*ISRM: Weibull-type conditional intensity function*

Since both confidence intervals for the parameters $\theta_{ij}$ contain the value 0, the interactions between the two subareas are not robust when using a Weibull-type c.i.f. Thus, the ISRM is applied—under appropriate restrictions—using a c.i.f. of the

form of Eq. (6) to fit separately data from the two subareas. The two curves are plotted in Fig. 11.

*SSRM: exponential and Weibull-type conditional intensity function*

The SSRM was applied for the entire central Ionian Islands area using the two types of the c.i.f. (Tables 5, 6, respectively). The AIC prefers the exponential c.i.f. for better fitting of the data, since the criterion favors the models with fewer parameters. The plots for the two different cases reveal similar behavior (Fig. 12).

**Fig. 12** The conditional intensity function versus time when applying the SSRM to the Central Ionian Islands using **a** an exponential-type c.i.f., **b** a Weibull-type c.i.f
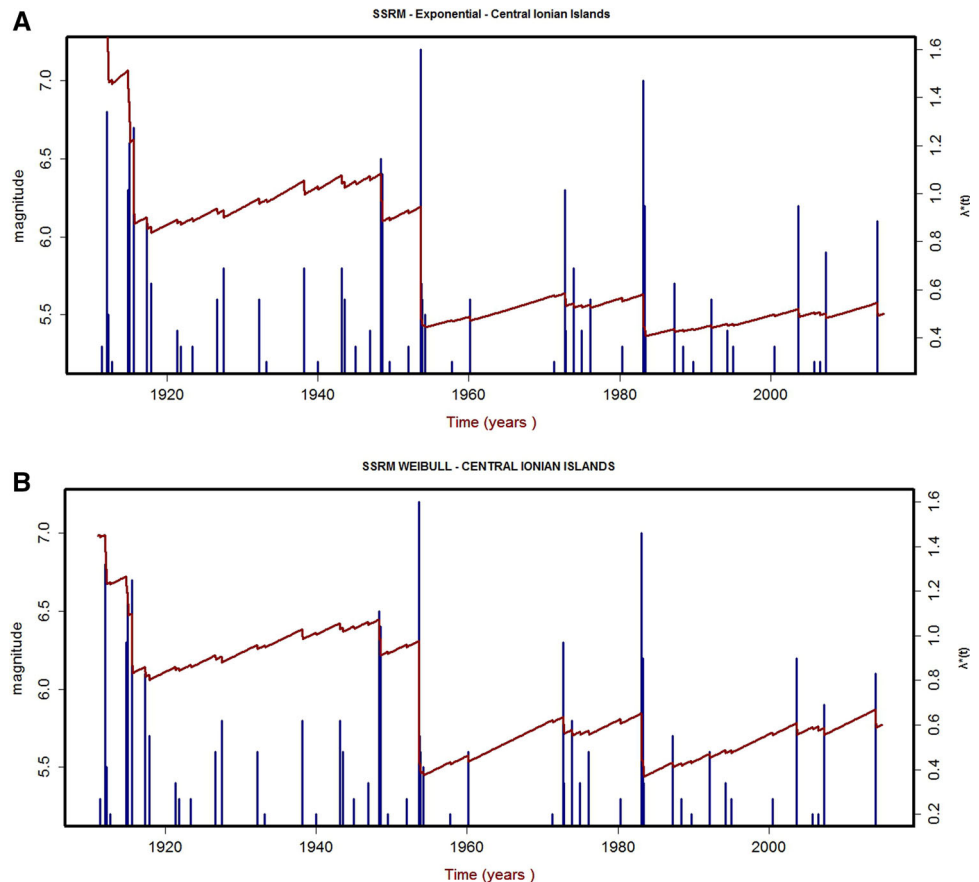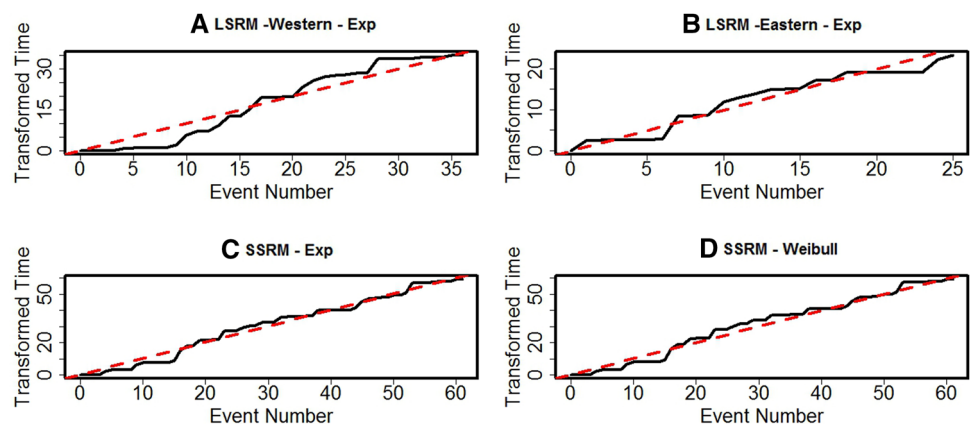


**Fig. 13** Residual analysis of **a** the LSRM for the western part of the Corinth Gulf using an exponential c.i.f., **b** the LSRM for the eastern part of the Corinth Gulf using an exponential c.i.f. **c** the SSRM using an exponential c.i.f. **d** the SSRM using a Weibull-type c.i.f



## Model fitting

For the model evaluation a residual analysis is performed (Ogata 1981). The goodness-of-fit of a point process model is tested using time transformation. The transformed process will be unit-rate Poisson, if the true model is adequately explained, whereas systematic deviation of the data from the fitted model would mean that an important feature is not yet included in the model. Residual analysis is performed to the models applied for both study areas. Figures 13 and 14 show some of the results for the sake of brevity. In general, the real number of events is in agreement with the number of events that emerges from the models. We should also notice that the results favor the use of the exponential c.i.f..

## Discussion and conclusions

In summary, despite its simplicity, the LSRM achieves to combine simple and basic ideas into a stochastic framework and could be taken into account as a first step towards the understanding of coupling and the interactions between

**Fig. 14** Residual analysis of **a** the LSRM for the subarea of Kefalonia using an exponential c.i.f. **b** the LSRM for the subarea of Lefkada using an exponential c.i.f. **c** the SSRM using an exponential c.i.f. **d** the SSRM using a Weibull-type c.i.f
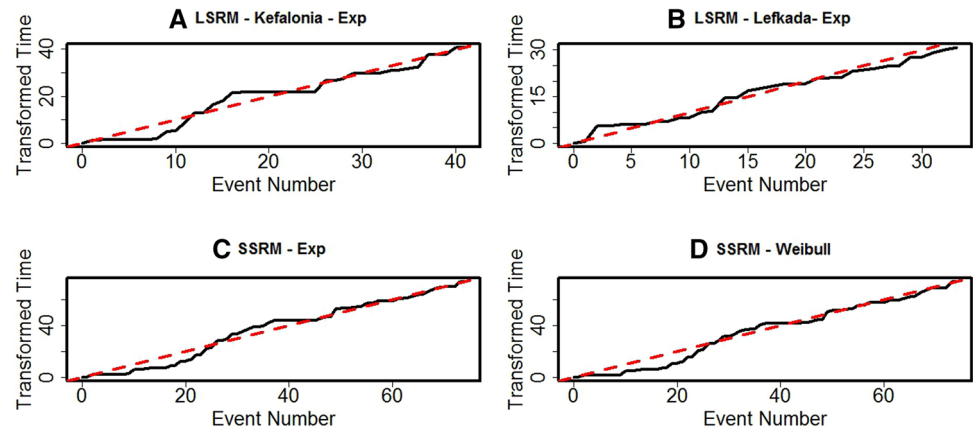


areas. It is applied to fit earthquake data from the Corinth Gulf and the central Ionian Islands areas, which are among the most seismically active ones in Europe. The behavior of the point process is determined by the conditional intensity function (c.i.f.). A Weibull-type c.i.f. is proposed, as a more flexible alternative than the one having an exponential-type. Although the curves are quite similar, the Akaike information criterion, which is used in order to evaluate competing models, in both cases clearly favors the use of the "classical" exponential form. The regionalization is an important aspect that arises when applying LSRM. In our case, the two study areas are divided based on seismotectonic criteria, comprise enough data for the numerical optimization to be e performed.

The interaction between different parts of an area is of major importance. An earthquake could accelerate or delay a second one, even at a quite distant area within a period of some years. Although the results do not reveal clearly the kind of interactions and the coupling between subareas, evidence is provided that the interactions imply damping from each subarea to another in both cases, the Corinth Gulf and central Ionian Islands. The motivation of finding out the style of interactions led to the application of the ISRM in the cases where the relation between earthquakes occurring in each subarea could not be proved.

The SSRM was applied in the western part of the Corinth Gulf by Rotondi and Varini (2006), and their results although based on different data samples and regionalization, are similar with ours regarding the shape and the trend of the conditional intensity functions. Our results regarding the central Ionian Islands are also comparable with those of Votsi et al. (2011) since both transfer parameters are found positive in both studies.

Particular attention was paid to computational issues. One of the main drawbacks of the maximum likelihood estimation (MLE) method, which is adopted for parameter estimation, is the sensitivity on the initial values used. The parameter space was scanned numerically using a dense

grid after taking also into account the model restrictions. These values were then used for examining the convergence and investigating the maximum of the log-likelihood function. Besides point estimation, interval estimation was also performed for the results to be more robust. The aim of stochastic modeling is the combination of both geophysical meaning and algorithm convergence.

## References

Akaike H (1974) A new look at the statistical model identification. IEEE Trans Autom Control 19(6):716–723

Aristotle University of Thessaloniki Seismological Network (1981) Permanent regional seismological network operated by the aristotle university of thessaloniki. International Federation of Digital Seismograph Networks. Other/ Seismic Network. doi:10.7914/SN/HT

Armijo R, Meyer B, King GCP, Rigo A, Papanastassiou D (1996) Quaternary evolution of the Corinth Rift and its implications for the late Cenozoic evolution of the Aegean. Geophys J Int 126:11–53

Bebbington M (2005) Information gains for stress release models. Pure Appl Geophys 162:2229–2319

Bebbington M, Harte D (2001) On the statistics of the linked stress release process. J Appl Probab 38:176–187

Bebbington M, Harte D (2003) The linked stress release model for spatio-temporal seismicity: formulations, procedures and applications. Geophys J Int 154:925–946

Borovkov K, Bebbington M (2003) A simple two-node stress transfer model reproducing Omori's law. Pure Appl Geophys 160:1429–1445

Bufe C, Varnes D (1993) Predictive modeling of the seismic cycle of the greater San Francisco bay region. J Geophys Res 98:9871–9883

Console R, Falcone G, Karakostas V, Murru M, Papadimitriou E, Rhoades D (2013) Renewal models and coseismic stress transfer in the Corinth Gulf Greece, fault system. J Geophys Res 118:3655–3673

Daley D, Vere-Jones D (2003) An introduction to the theory of point processes, vol 1, 2nd edn. Springer, New York, pp 211–287

Gabrielov A, Newman WI (1994) Seismicity modelling and earthquake prediction: a review. In: Newman WI, Gabrielov A, Turcotte DL (eds) Nonlinear dynamics and predictability of geophysical phenomena. Am Geophys Union, Washington, DC, pp 7–13

Harte DS, Vere-Jones D (2005) The entropy score and its uses in earthquake forecasting. Pure Appl Geophys 162:1229–1253

Imoto M, Hurukawa N (2006) Assessing potential seismic activity in Vrancea, Romania, using a stress-release model. Earth Planets Space 58:1511–1514

Isham V, Westcott M (1979) A self-correcting point process. Stoch Process Appl 8:335–347

Jackson JA, White NJ (1989) Normal faulting in the upper continental crust: observations from regions of active extension. J Struct Geol 11:15–36

Jiang M, Zhu S, Chen Y, Ai Y (2011) A new multidimensional stress release statistical model based on coseismic stress transfer. Geophys J Int 187:1479–1494

Kagan Y, Jackson D (1991) Long-term earthquake clustering. Geophys J Int 104:117–133

Kanamori H, Anderson DL (1975) Theoretical basis of some empirical relations in seismology. Bull Seismol Soc Am 65(5):1073–1095

Liu J, Vere-Jones D, Ma L, Shi Y, Zhuang JC (1998) The principal of coupled stress release model and its application. Acta Seismologica Sinica 11:273–281

Liu C, Chen Y, Shi Y, Vere-Jones D (1999) Coupled stress release model for time-dependent seismicity. Pure Appl Geophys 155:649–667

Lu C (2005) The degree of predictability of earthquakes in several regions of China: statistical analysis of historical data. J Asian Earth Sci 25:379–385

Lu C, Vere-Jones D (2000) Application of linked stress release model to historical earthquake data: comparison between two kinds of tectonic seismicity. Pure Appl Geophys 157:2351–2364

Lu C, Vere-Jones D (2001) Statistical analysis of synthetic earthquake catalogs generated by models with various levels of fault zone disorder. J Geophys Res 106(B6):11115–11125

Lu C, Harte D, Bebbington M (1999) A linked stress release model for historical Japanese earthquakes: coupling among major seismic regions. Earth Planets Space 51:907–916

Ogata Y (1981) On Lewis's simulation method for point processes. IEEE Trans Inf Theory 27:23–31

Papadimitriou EE (2002) Mode of strong earthquake recurrence in the Central Ionian Islands (Greece): possible triggering due to Coulomb stress changes generated by the occurrence of previous strong shocks. Bull Seismol Soc Am 92(8):3293–3308

Papazachos BC, Papazachou CC (2003) The earthquakes of Greece. Ziti Publications, Thessaloniki

Papazachos BC, Karakaisis GF, Papadimitriou EE, Papaioannou ChA (1997) Time dependent seismicity in the Alpine-Himalayan belt. Tectonophys 271:295–324

Reid H (1910) The mechanics of the earthquake, The California earthquake of april 18, 1906. Report of the state investigation commission, vol 2. Carnegie Institution of Washington, Washington, DC, pp 16–28

Rotondi R, Varini E (2006) Bayesian analysis of marked stress release models for time-dependent hazard assessment in the western Gulf of Corinth. Tectonophys 423:107–113

Rotondi R, Varini E (2007) Bayesian inference of stress release models applied to some seismogenic zones. Geophys J Int 169:301–314

Scordilis EM, Karakaisis GF, Karakostas BG, Panagiotopoulos DG, Comninakis PE, Papazachos BC (1985) Evidence for transform faulting in the Ionian Sea: The Cephalonia island earthquake sequence of 1983. Pure Appl Geophys 123:388–397

Varini E, Rotondi R (2015) Probability distribution of the waiting time in the stress release model: the Gompertz distribution. Environ Ecol Stat 22:493–511

Vere-Jones D (1978) Earthquake prediction-a statistician's view. J Phys Earth 26(2):129–146

Vere-Jones D, Deng YL (1988) A point process analysis of historical earthquakes from North China. Earthq Res China 2:165–181

Votsi I, Tsaklidis G, Papadimitriou E (2011) Seismic hazard assessment in Central Ionian Islands Area based on stress release models. Acta Geophys 59:701–727

Wessel P, Smith WHF (1998) New, improved version of the generic mapping tools released. Trans Am Geophys Union 79:579

Zheng X, Vere-Jones D (1994) Further applications of the stochastic stress release model to historical earthquake data. Tectonophys 229:101–121